

# eIF4E-bound mRNPs are substrates for nonsense-mediated mRNA decay in mammalian cells

Simone C Rufener<sup>1,2</sup> & Oliver Mühlemann<sup>1</sup>

**Eukaryotic mRNAs with premature translation termination codons (PTCs) are recognized and degraded through a process termed nonsense-mediated mRNA decay (NMD). The evolutionary conservation of the core NMD factors UPF1, UPF2 and UPF3 implies a similar basic mechanism of PTC recognition in all eukaryotes. However, while PTC-containing mRNAs in yeast seem to be available to NMD at each round of translation, mammalian NMD has been reported to be restricted to cap-binding complex (CBC)-bound mRNAs during the pioneer round of translation. Here, we compared decay kinetics of two NMD reporter genes in mRNA fractions bound to either CBC or the eukaryotic initiation factor 4E (eIF4E) in human cells and demonstrate that NMD destabilizes eIF4E-bound transcripts as efficiently as those associated with CBC. These results corroborate an emerging unified model for NMD substrate recognition, according to which NMD can ensue at every aberrant translation termination event.**

During gene expression in eukaryotes, newly synthesized mRNA transcripts undergo a series of processing steps and assemble with a set of RNA-binding proteins to form highly compact mRNA ribonucleoprotein particles (mRNPs) before their release into the cytoplasm, where they serve as templates for protein synthesis<sup>1,2</sup>. During transcription, the co-transcriptionally formed 7-methylguanylate cap at the 5' end of each mRNA is bound by the cap-binding complex (CBC), a heterodimer consisting of the proteins CBP80 and CBP20 (refs. 3,4). Another prominent component of spliced mRNPs is the exon junction complex (EJC), which is deposited as a consequence of pre-mRNA splicing 20–24 nucleotides (nt) upstream of most exon-exon junctions in mammalian cells<sup>2,5,6</sup>. Moreover, several hundred additional mRNA binding proteins have been identified that interact with different mRNA species at variable stoichiometries<sup>7,8</sup>. Influenced by transcript sequence and cellular environment, the protein composition of an mRNP is highly dynamic and affects its splicing, export, stability, localization and translation, thereby contributing to the regulation and coordination of the complex post-transcriptional gene expression networks<sup>9</sup>.

After mRNPs are exported to the cytoplasm, they engage with ribosomes and can undergo their initial round of translation while still bound to the CBC<sup>10–12</sup>. This first round of translation might even begin before the entire mRNP has been extruded from the nuclear pore<sup>13</sup>. Translation induces extensive rearrangements of the CBC-bound mRNPs<sup>11,14,15</sup>. EJCs and EJC-associated factors are removed by the translating ribosomes<sup>15,16</sup>, and the exchange of nuclear poly(A)-binding protein N1 (PABPN1) with cytoplasmic PABPC1 at the poly(A) tail also appears to be promoted by translation<sup>14</sup>. In contrast, the replacement of CBC by eIF4E occurs in a translation-independent manner, by a mechanism that involves

the karyopherin importin- $\beta$ -promoted dissociation of CBC from the mRNA<sup>14,17,18</sup>. CBC dissociation permits binding of the cap by eIF4E, which on its own has a lower affinity to the cap than CBC<sup>19,20</sup>. Together with eIF4A and eIF4G, which strengthen the interaction between eIF4E and the cap, eIF4E forms the eIF4F translation initiation complex, which then supports the bulk of cellular protein synthesis<sup>21,22</sup>.

Several quality-control mechanisms contribute to ensuring sufficient accuracy of gene expression for proper cell function and viability. NMD is one of these surveillance mechanisms. NMD recognizes and degrades mRNAs harboring a termination codon in an unfavorable environment for efficient translation termination<sup>23,24</sup>. The exact conditions determining whether a translation termination event activates NMD are not yet fully understood. It is thought that in the absence of an interaction between PABPC1 and eukaryotic release factor 3 (eRF3), the central NMD factor up-frameshift 1 (UPF1) instead binds to eRF3 at the stalled ribosome and, together with the phosphoinositide-3-kinase (PIK)-related protein kinase SMG1, forms the SMG1-UPF1-release factor (SURF) complex<sup>25,26</sup>. The subsequent interaction of UPF2 and UPF3B with UPF1 and SMG1 induces a conformational change of the complex, which stimulates the SMG1-catalyzed phosphorylation of UPF1 (refs. 25,27–29). UPF1 phosphorylation is essential for mammalian NMD and is believed to commit the associated mRNA to rapid degradation through the recruitment of SMG6, the heterodimer SMG5-SMG7 and/or proline-rich nuclear receptor co-regulatory protein 2 (refs. 27,30–32).

In mammalian cells, NMD has been reported to act exclusively on newly synthesized CBC-bound transcripts during the 'pioneer round of translation'. At this initial stage of translation, it has been proposed that one or few ribosomes act as proofreaders, triggering NMD and

<sup>1</sup>Department of Chemistry and Biochemistry, University of Bern, Bern, Switzerland. <sup>2</sup>Graduate School for Cellular and Biomedical Sciences, University of Bern, Bern, Switzerland. Correspondence should be addressed to O.M. (oliver.muehlemann@dcb.unibe.ch).

Received 24 January; accepted 4 April; published online 12 May 2013; doi:10.1038/nsmb.2576

hence eliminating faulty transcripts early on, before they undergo eIF4E-associated bulk translation<sup>11,12,33,34</sup>. Several lines of evidence indicate that mammalian NMD acts on CBC-bound mRNAs: (i) the abundance of CBP80-associated nonsense mRNA is reduced relative to the corresponding CBP80-associated wild-type transcript<sup>11</sup>, (ii) the NMD factors UPF1, UPF2, UPF3 and SMG1 have been detected in CBC-associated mRNPs<sup>11,15,25,35</sup>, and (iii) knockdown of CBP80 and the CBC-interacting protein CTIF partially inhibits NMD<sup>35,36</sup>. Moreover, CBP80 has been reported to interact with UPF1 and thereby promote SURF complex formation<sup>34,35</sup>. Although the evidence for NMD targeting nonsense mRNAs during the pioneer round of translation is strong, direct evidence demonstrating that eIF4E-associated mRNAs are immune to NMD is lacking. In fact, evidence for the restriction of NMD to CBC-bound mRNA is based largely on negative results. For example, inhibition of eIF4E-mediated translation by overexpression of the 4E-binding protein 1, prolonged hypoxia or serum starvation did not inhibit NMD<sup>12,37,38</sup>. Nevertheless, restriction of NMD to the CBC-associated pioneer round of translation has been strongly advocated<sup>33,39,40</sup>.

The recently reported evidence for a translation-independent exchange of CBC with eIF4E at the cap<sup>14</sup>, and the finding that NMD can be antagonized by retroviral RNA elements that promote translational read-through at very low frequency<sup>41</sup>, challenge the model of NMD restriction to the CBC-associated pioneer round of translation. Moreover, the evolutionary conservation of UPF1, UPF2 and UPF3 suggests a conserved basic NMD mechanism among all eukaryotes, and in *Saccharomyces cerevisiae*, NMD is not limited to early rounds of translation<sup>42–44</sup>.

To address whether eIF4E-bound transcripts are indeed immune to NMD in human cells, we determined the mRNA half-lives of immunopurified mRNPs bound to CBP80 and eIF4E. Our results demonstrate that NMD acts efficiently both on CBP80- and 4E-bound transcripts. Furthermore, our results indicate that the cap-binding protein, probably in combination with other differentially associated mRNP components, influences the general turnover rate of the associated mRNA.

## RESULTS

### RNA-mediated interaction of UPF1 with CBP80 and eIF4E

To re-investigate the reported restriction of mammalian NMD to CBC-bound mRNAs<sup>11,12,36</sup>, we established an efficient protocol for isolating mRNPs that are associated with either endogenous CBP80 or eIF4E. We performed immunoprecipitations using an antibody to CBP80 (anti-CBP80) or anti-eIF4E in HeLa cell extracts in the presence or absence of RNase A, and we used normal IgG as a negative control. The immunopurified proteins were subjected to western blotting and examined for the presence of CBP80, CBP20, eIF4E, UPF1, PABPC1, eIF4G and  $\beta$ -actin (**Fig. 1**). Confirming the well-established direct interaction between CBP80 and CBP20 (refs. 3,45), CBP20 co-purified with CBP80 in an RNase A-resistant manner (**Fig. 1a**, lanes 4 and 6). UPF1 and PABPC1 also co-purified with CBP80 in the absence of RNase A, but these interactions were lost when the extracts were treated with RNase A before immunoprecipitation, indicating that they are RNA-mediated (**Fig. 1a**, lanes 4 and 6). Consistently, endogenous CBP80 co-precipitated with Flag-tagged PABPC1 (Flag-PABPC1) and Flag-UPF1 only in the absence of RNase A (**Supplementary Fig. 1a** and **Supplementary Note**). The RNase-sensitivity of the CBP80-UPF1 interaction is consistent with data from a previous study<sup>27</sup>, but inconsistent with the reported interaction between the C-terminal region of CBP80 and a part of the UPF1 helicase domain<sup>34</sup>. The RNase sensitivity of the

CBP80-PABPC1 interaction, and the apparent absence of eIF4GI in the CBP80 precipitate, suggests that CBC-bound mRNAs probably lack mRNP circularization analogous to the well-characterized eIF4E-eIF4G-PABPC1 interaction that brings the 5' and 3' ends of mRNAs close together<sup>46,47</sup>. This is further supported by the loss of the interaction of CBP80 with Flag-PABPN1 and Flag-PABPC1 upon RNase A digestion (**Supplementary Fig. 1a**). We confirmed the effectiveness of the RNase A treatment by reverse transcription PCR (RT-PCR) analysis of stably expressed TCR- $\beta$  reporter mRNA (**Fig. 1c**).

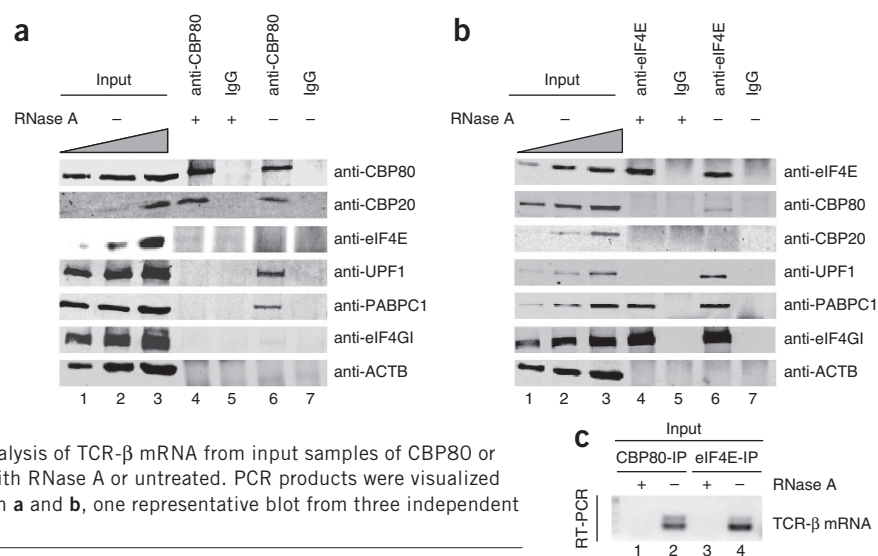
While we cannot rule out the presence of small amounts of eIF4G (below our detection limit) in the CBP80 immunoprecipitations, the absence of eIF4G in CBC-associated mRNPs would be consistent with a previous study characterizing a CBP80/20-dependent translation initiation factor (CTIF) that replaces eIF4G in translation initiation of CBC-associated mRNA<sup>36</sup>. However, those and our data are inconsistent with the reported direct interaction between CBP80 and eIF4G and the proposed function of eIF4G during the pioneer round of translation<sup>12,48,49</sup>. Additionally, CTIF was readily detectable in our input samples but not in any of our CBP80 immunoprecipitations (**Supplementary Fig. 1b**). As expected, and confirming the specificity of the immunoprecipitation, eIF4E and  $\beta$ -actin were not detectable in the CBP80 immunoprecipitates, and none of the tested proteins were present in the control immunoprecipitations.

In contrast to the relatively low immunoprecipitation efficiency achieved with anti-CBP80 (even under optimized conditions, only ~5% of the total cellular CBP80 could be purified), 40% of the total cellular eIF4E protein was precipitated by the eIF4E immunoprecipitation (data not shown). We also confirmed the above-mentioned mRNA-circularizing eIF4E-eIF4G-PABPC1 interaction (**Fig. 1b**, lanes 4 and 6). Notably, UPF1 also co-purified with eIF4E-associated mRNPs in an RNA-dependent manner (**Fig. 1b**, lanes 4 and 6), in contrast to previous studies that did not detect UPF1 associated with eIF4E-bound mRNA<sup>11,35</sup>. We confirmed this RNA-dependent interaction by reverse immunoprecipitations of Flag-UPF1 (**Supplementary Fig. 1a**). Additionally, a very weak CBP80 signal was sometimes observed in the eIF4E immunoprecipitates when the lysates were not treated with RNase A. However, this interaction was no longer detected when the cells were lysed in a more stringent lysis buffer containing more detergent and a higher salt concentration, whereas UPF1 could still be detected under these conditions (**Supplementary Fig. 1c**). Moreover, we did not detect CBP20, which forms a stable heterodimer with CBP80, in eIF4E immunoprecipitations under any condition, indicating that the minute amount of CBP80 detected at lower stringency represents an unspecific, low-affinity contamination. We did not detect  $\beta$ -actin, which was used as negative control, in the eIF4E immunoprecipitations, and none of the tested proteins were present in the IgG control immunoprecipitation.

### Rapid decay of NMD reporter mRNA bound to CBP80 and eIF4E

After detection of UPF1 in mRNPs associated with CBP80 (CBC-mRNPs) and with eIF4E (4E-mRNPs), we hypothesized that NMD could also target eIF4E-bound mRNAs, as has been shown in *S. cerevisiae*<sup>42–44</sup>. If NMD is restricted to the pioneer round of translation (that is, if NMD exclusively targets CBP80-bound transcripts), the half-lives ( $t_{1/2}$ ) should be similar for eIF4E-bound mRNAs that contain PTCs (PTC+) and those that do not (wild type), whereas CBP80-bound PTC+ mRNA would be degraded faster than the CBP80-associated wild-type transcripts. In contrast, if eIF4E-bound mRNAs can also be targeted by NMD, a similar  $t_{1/2}$  reduction of eIF4E-bound PTC+ transcripts (relative to  $t_{1/2}$  of wild type) would be expected, as for CBP80-bound PTC+ transcripts.

**Figure 1** Immunopurification of CBC- and eIF4E-mRNPs. **(a)** UPF1 and PABPC1 co-immunopurify with CBP80 in an RNA-dependent manner. Lysates from HeLa Tet-Off cells expressing TCR- $\beta$  wild-type mRNA and treated with RNase A (+) or untreated (-) were immunopurified using anti-CBP80 or normal rabbit IgG (negative control) and subjected to western blotting using the antibodies indicated, before (input) or after immunoprecipitation. Lanes 1–3 represent 1%, 2% and 4% of the input, respectively. Lanes 4–7 represent 50% of the immunoprecipitated material. **(b)** UPF1 is present in 4E-mRNPs. Immunoprecipitations were performed as in **a**, using anti-eIF4E antibody or normal mouse IgG (negative control). Lanes 4–7 represent 25% of the immunoprecipitated material. **(c)** RT-PCR analysis of TCR- $\beta$  mRNA from input samples of CBP80 or eIF4E immunoprecipitation experiments, treated with RNase A or untreated. PCR products were visualized on an agarose gel stained with ethidium bromide. In **a** and **b**, one representative blot from three independent experiments is shown. ACTB,  $\beta$ -actin.



To distinguish between these two scenarios, we purified CBC-mRNPs and 4E-mRNPs from cells expressing TCR- $\beta$  reporter mRNA—either wild type or with a PTC at amino acid position 68 (ter68; **Fig. 2a**)—and determined  $t_{1/2}$  for each transcript. TCR- $\beta$  ter68 is a classical NMD target in which an EJC is predicted to reside on the mRNA sufficiently downstream of the PTC to function as a NMD enhancer during translation termination<sup>24</sup>. To confirm that observed  $t_{1/2}$  reductions were caused by NMD, we performed the experiment under UPF1-knockdown and control conditions (achieved by expression of a short hairpin RNA (shRNA) with a scrambled target sequence). To measure  $t_{1/2}$ , we used HeLa Tet-Off cells, in which transcription of the TCR- $\beta$  reporter genes is blocked in the presence of doxycycline<sup>50</sup>. Cell extracts from each time point after transcription shut-off were divided and subjected to immunoprecipitations with anti-CBP80 or anti-eIF4E, with IgG as a control. From the immunoprecipitated material, we generated protein extracts for western blotting (**Fig. 2b**) and isolated RNA for analysis by reverse transcription–quantitative PCR (RT-qPCR; **Fig. 2c–h**).

Compared to control conditions (**Fig. 2b**, lanes 1–3), UPF1 knockdown reduced UPF1 protein abundance by about 90% in whole-cell extract, over the entire time course of the experiment (**Supplementary Fig. 2a**). Notably, residual amounts of UPF1 were still detectable in 4E-mRNPs under UPF1-knockdown conditions, but not in CBC-mRNPs (**Fig. 2b**, lanes 6 and 9). UPF1 knockdown did not affect the association of PABPC1 with CBC-mRNPs and 4E-mRNPs or of eIF4GI with 4E-mRNPs. As in the previous experiment (**Fig. 1a**), we did not detect eIF4GI in CBC-mRNPs (**Fig. 2b**, lanes 5 and 6). To determine decay kinetics of the TCR- $\beta$  NMD reporter transcripts in the CBC-mRNP and the 4E-mRNP fractions, we measured relative TCR- $\beta$  mRNA levels by RT-qPCR in samples from our time-course experiment. TCR- $\beta$  RNA levels were normalized to endogenous  $\beta$ -actin mRNA levels to account for potential variability among the different immunoprecipitations (**Fig. 2c,d**). The levels of  $\beta$ -actin mRNA and the amounts of CBP80 and eIF4E protein varied only slightly among samples from different time points, demonstrating comparable immunoprecipitation efficiencies throughout the time course. In the control samples,  $\beta$ -actin mRNA levels were, on average, 4% and 2% of the levels measured in the CBP80 and eIF4E immunoprecipitations, respectively (**Fig. 2c,d**, compare lanes 1–4 with lane 5), demonstrating the high enrichment

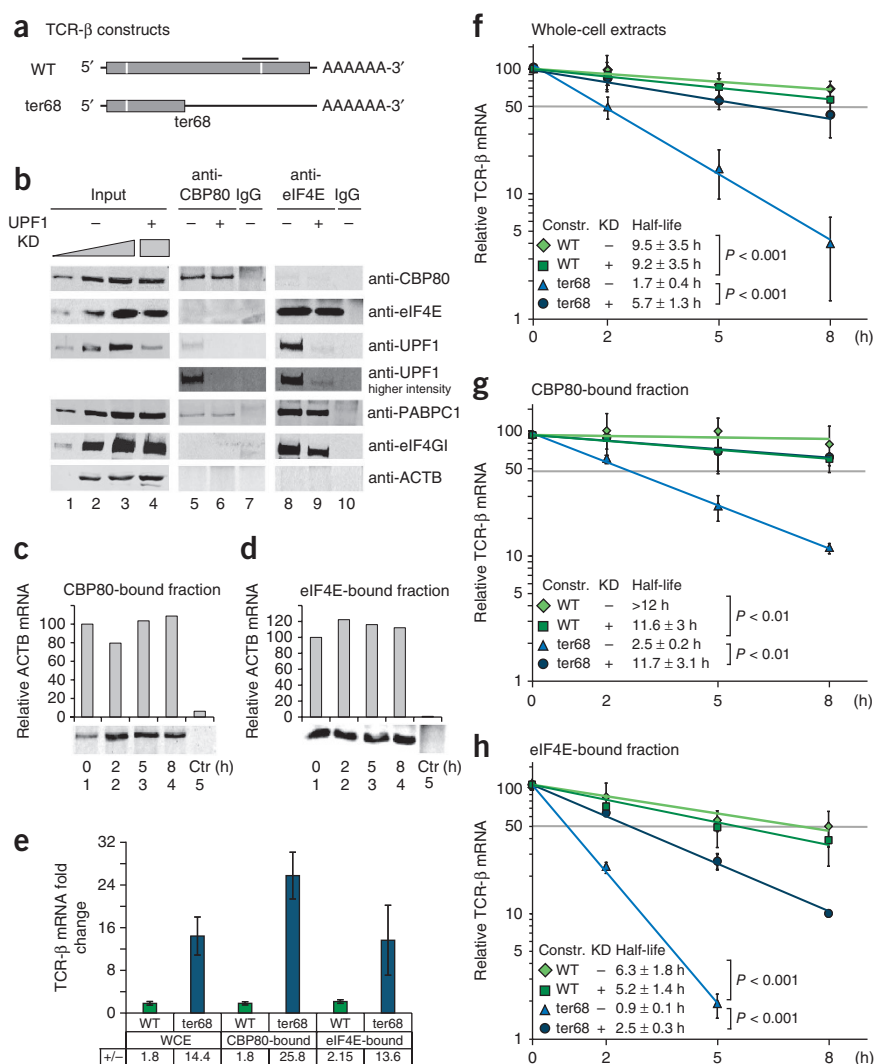
of mRNA in the CBP80 and eIF4E immunoprecipitates. To specifically examine decay kinetics of the mRNA pool produced before transcription inhibition, we determined the background expression originating from slight leakiness of the Tet-Off system in each cell line and subtracted it from the relative mRNA level at every time point (**Supplementary Fig. 2e,f**).

On the basis of at least three independent experiments,  $t_{1/2}$  for TCR- $\beta$  ter68 mRNA in whole-cell extracts was  $5.7 \pm 1.3$  h upon UPF1 knockdown (compared to  $1.7 \pm 0.4$  h in controls; mean  $\pm$  s.d. of  $\geq 3$  independent experiments), whereas  $t_{1/2}$  for TCR- $\beta$  wild-type mRNA was not significantly affected by UPF1 knockdown ( $9.5 \pm 3.5$  h versus  $9.2 \pm 3.5$  h;  $P > 0.3$ ; **Fig. 2f**). This result confirms that TCR- $\beta$  ter68 is a robust NMD substrate. In comparison,  $t_{1/2}$  for the CBP80-associated fraction of TCR- $\beta$  ter68 mRNA was  $2.5 \pm 0.2$  h and stabilized to  $11.7 \pm 3.1$  h upon UPF1 knockdown, a value indistinguishable from  $t_{1/2}$  for TCR- $\beta$  wild-type mRNA under the same conditions ( $11.6 \pm 3$  h, **Fig. 2g**). This result is consistent with previous studies demonstrating that NMD targets CBC-bound mRNA<sup>11,12,34,36</sup>. Notably, the  $t_{1/2}$  of the eIF4E-associated TCR- $\beta$  ter68 mRNA was  $0.9 \pm 0.1$  h under control conditions and increased to  $2.5 \pm 0.3$  h upon UPF1 knockdown, strongly indicating that the eIF4E-associated TCR- $\beta$  ter68 transcripts are also degraded by NMD (**Fig. 2h**). The observed stabilization of eIF4E- and CBP80-bound TCR- $\beta$  ter68 mRNA upon NMD attenuation suggests that TCR- $\beta$  ter68 mRNA is efficiently targeted by NMD, irrespectively of whether its cap structure is bound by CBC or eIF4E.

The UPF1 knockdown–mediated stabilization of TCR- $\beta$  ter68 transcripts was also manifest as higher steady-state TCR- $\beta$  ter68 mRNA levels in all three categories (whole-cell extract, CBP80-bound fraction and eIF4E-bound fraction). The mRNA increase was highest in the CBC-mRNP fraction (26-fold higher than in control-knockdown conditions) and somewhat less pronounced in whole-cell extracts and the 4E-mRNP fraction ( $\sim 14$ -fold for both; **Fig. 2e**). The larger increase of TCR- $\beta$  ter68 mRNA in the CBC-mRNP fraction suggests that NMD of CBC-associated mRNA is more sensitive than NMD of eIF4E-associated mRNA to lowered UPF1 levels (see Discussion).

Notably, the  $t_{1/2}$  values for both TCR- $\beta$  transcripts—wild type and ter68—were significantly shorter for mRNAs associated with eIF4E than for those bound to CBP80, under UPF1- and control-knockdown conditions (wild type under control-knockdown

**Figure 2** CBP80- and eIF4E-associated PTC-containing TCR- $\beta$  mRNAs are NMD targets. (a) Schematic of TCR- $\beta$  wild-type and ter68 mRNAs. The black bar indicates the fragment amplified in the qPCR assay in e–h. (b–h) TCR- $\beta$  wild-type- or ter68-expressing HeLa Tet-Off cells subject to knockdown (KD) of UPF1 or control KD were incubated with doxycycline for 0, 2, 5 or 8 h. From each time point, RNPs were immunopurified from whole-cell extracts (WCEs) using anti-CBP80 or anti-eIF4E antibody. Control immunoprecipitations with normal IgG (Ctr) were performed with doxycycline-treated cells after 8 h. Relative TCR- $\beta$  mRNA levels, normalized to endogenous  $\beta$ -actin mRNA, were determined by RT-qPCR from WCEs or CBP80- or eIF4E-associated fractions. Western blots (b) were done to assess protein composition of immunopurified mRNPs and efficacy of the UPF1 KD. Lanes 1–3 represent 0.5%, 1.5% and 4.5% of the input from the control KD (–), respectively; lane 4 represents 4.5% of input from the UPF1 KD cells (+) and lanes 5–10 represent 50% of the immunoprecipitated material. CBP80 (c) or eIF4E (d) immunoprecipitation efficiencies throughout the time course documented by immunopurified endogenous  $\beta$ -actin mRNA and western blots showing CBP80 or eIF4E, respectively. Average ratios ( $\pm$  s.d.) of normalized TCR- $\beta$  mRNA levels after UPF1 and control KD (+/–) at time point 0 show the increase of TCR- $\beta$  ter68 mRNA upon UPF1 KD in all fractions ( $n \geq 3$ ) (e). Half-lives and s.d. of TCR- $\beta$  transcripts (f–h) were calculated from  $\geq 3$  independent experiments (Online Methods). ACTB,  $\beta$ -actin; constr., construct; WT, wild type.



conditions,  $P < 0.05$ ; wild type under UPF1-knockdown conditions,  $P < 0.01$ ; ter68 under control-knockdown conditions,  $P < 0.001$ ; ter68 under UPF1-knockdown conditions,  $P < 0.001$ ). This might represent a generally faster turnover rate of mRNAs engaged in eIF4E-mediated translation (Fig. 2g,h). Reassuringly,  $t_{1/2}$  values for mRNAs from whole-cell extracts always fell between the  $t_{1/2}$  values for each mRNA fraction, consistent with whole-cell extract representing the merge of both fractions (Fig. 2f).

Because reassociation of RNA-binding proteins after cell lysis is a well-known pitfall of RNA immunoprecipitation experiments<sup>51</sup>, we wondered whether eIF4E could have partially replaced CBC in the cellular extracts or during immunoprecipitation, although this seemed highly unlikely in light of compelling evidence demonstrating a much tighter binding of CBC to the cap structure than eIF4E—the overall equilibrium association constant of the cap analog m<sup>7</sup>GpppG binding to CBC is two orders of magnitude higher than that of m<sup>7</sup>GpppG binding to eIF4E<sup>19,20</sup>. Nevertheless, to exclude the possibility that the TCR- $\beta$  ter68 mRNA we measured in the eIF4E immunoprecipitations could have undergone NMD while bound by CBP80 *in vivo* and then been replaced by eIF4E after cell lysis, we repeated the eIF4E immunoprecipitation time-course experiment with cells that were cross-linked with formaldehyde before cell lysis (Supplementary Fig. 3). We obtained almost the same result from this experiment as from the previous experiments without cross-linking. Hence, we conclude that the cellular pool of eIF4E-associated mRNAs can be degraded by NMD.

### Efficient NMD of eIF4E-bound transcripts with long 3' UTRs

Rescue of the eIF4E-bound TCR- $\beta$  ter68 transcripts upon UPF1 knockdown was only partial, indicating that some eIF4E-bound mRNAs are still degraded by residual NMD activity under UPF1-knockdown conditions that completely block NMD of CBC-bound transcripts. This could be a result of different translation efficiencies of CBC-mRNPs and 4E-mRNPs. During eIF4E-mediated bulk translation, the same mRNA molecule is translated multiple times, and UPF1 might therefore have multiple chances to trigger NMD, resulting in residual NMD activity even at low UPF1 concentrations. In contrast, the presumably fewer rounds of translation of a CBC-associated mRNA present fewer opportunities for residual UPF1 to induce NMD, resulting in more efficient stabilization of the mRNA under knockdown conditions. This hypothesis is underlined by the residual amounts of UPF1 present in 4E-mRNPs but not CBC-mRNPs under UPF1-knockdown conditions (Fig. 2b, lanes 6 and 9). Therefore, we sought ways to inhibit NMD by means other than knockdown of NMD factors.

We decided to repeat the mRNA fractionation time-course experiments with HeLa Tet-Off cells stably expressing a set of previously described NMD reporter constructs derived from a gene encoding mouse immunoglobulin- $\mu$  (mini $\mu$ )<sup>50</sup>. The parental mini $\mu$  wild-type 'no foldback' mRNA (NFB) is converted into an NMD substrate by

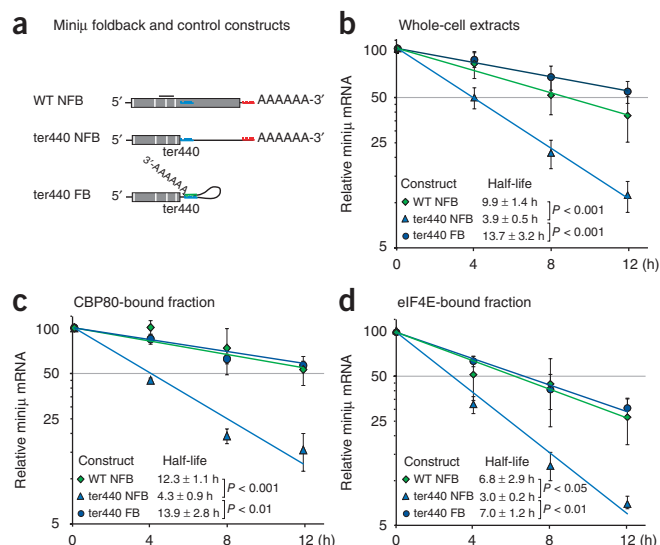


**Figure 3** CBP80- and eIF4E-associated PTC+ miniµ reporter mRNA is rapidly degraded by NMD when the poly(A) tail is distant from the PTC. (a) Schematic of miniµ reporter mRNAs. Wild-type NFB has the full-length ORF, and ter440 NFB has a PTC at codon 440 and is an NMD substrate<sup>50</sup>. A 26-nt sequence downstream of codon 440 is highlighted in blue. In the NFB constructs, the identical sequence was inserted upstream of the poly(A) tail (depicted in red), whereas in the ter440 FB construct, the complementary sequence (green) was inserted, allowing the poly(A) tail to fold back into the proximity of ter440, which suppresses NMD<sup>50</sup>. The position of the fragment amplified in the qPCR assays described in b–d is indicated by a black bar. (b–d) Rapid degradation by NMD of ter440 NFB in whole-cell extracts (WCEs) or CBP80- and eIF4E-bound mRNA fractions. HeLa Tet-Off cells stably expressing constructs described in a were exposed to doxycycline for 0, 4, 8 or 12 h. From WCEs taken at each time point, CBP80 and eIF4E immunoprecipitations were performed as described in Figure 1a, and miniµ mRNA from WCEs and co-purified fractions was analyzed by RT-qPCR as in Figure 2. Half-lives and  $\pm$  s.d. were calculated from  $\geq 3$  independent experiments (Online Methods). WT, wild type.

a point mutation that introduces a PTC at amino acid position 440 (ter440 NFB; Fig. 3a). NMD of ter440 transcripts can be suppressed by the insertion immediately upstream of the poly(A) signal of a 26-nt sequence that is complementary to the sequence located ~50 nt downstream of the PTC (the resulting mRNA is termed ter440 ‘fold-back’ (ter440 FB) mRNA)<sup>50</sup>. Base pairing of these complementary sequences positions the poly(A) tail in close proximity to the PTC, thereby restoring PABP-mediated proper translation termination and suppression of NMD<sup>26,50</sup>. Notably, the insertion of this sequence has no effect on the expression level and decay kinetics of the miniµ wild-type NFB construct<sup>50</sup>. Another feature of the ter440 NFB construct is the absence of an intron downstream of the PTC. Unlike TCR- $\beta$  ter68, ter440 NFB mRNA is degraded by an EJC-independent mode of NMD<sup>24,52</sup>.

We determined, from at least three independent time-course experiments, a  $t_{1/2}$  for ter440 NFB of  $3.9 \pm 0.5$  h in whole-cell extracts (Fig. 3b). For ter440 FB,  $t_{1/2}$  was  $13.7 \pm 3.2$  h, similar to  $t_{1/2}$  for wild-type NFB ( $9.9 \pm 1.4$  h). In the CBC-mRNP fraction, ter440 FB also completely suppressed NMD, with a  $t_{1/2}$  of  $13.9 \pm 2.8$  h, which is similar to the  $t_{1/2}$  of wild-type NFB ( $12.3 \pm 1.1$  h; Fig. 3c). Again, we noted that in the 4E-mRNP fraction, all three reporter mRNAs decayed significantly faster than in the CBC-mRNP fraction (Fig. 3c,d) (ter440 NFB,  $P < 0.05$ ; ter440 FB,  $P < 0.01$ ; wild-type NFB,  $P < 0.05$ ). For

the NMD-sensitive ter440 NFB transcript,  $t_{1/2}$  was  $3.0 \pm 0.2$  h in the 4E-mRNP fraction. Notably,  $t_{1/2}$  of ter440 FB was increased to  $7.0 \pm 1.2$  h, which is very similar to the  $t_{1/2}$  of the wild-type NFB control transcript ( $6.8 \pm 2.9$  h) and indicates complete NMD suppression (Fig. 3d).

## DISCUSSION

Collectively, our results demonstrate that NMD can efficiently target eIF4E-bound mRNAs as well as mRNAs bound to CBC in human cells. First, we showed that UPF1 co-precipitates with eIF4E in an RNA-dependent manner, demonstrating the presence of UPF1 in 4E-mRNPs (Fig. 1b). Second and most notably, eIF4E-associated nonsense-containing TCR- $\beta$  and miniµ transcripts are efficiently degraded by NMD, as reflected in the fast decay rate of PTC+ transcripts associated with eIF4E (Figs. 2h and 3d) and the recovery of  $t_{1/2}$  values for ter440 FB transcripts that are comparable to  $t_{1/2}$  values for wild-type NFB transcripts in eIF4E-associated mRNA fractions (Fig. 3d). UPF1 knockdown resulted in full recovery of CBC-associated PTC-containing transcripts, whereas  $t_{1/2}$  for eIF4E-bound mRNAs was only partially recovered upon UPF1 knockdown (Fig. 2). This observation suggests that CBC-associated NMD is more sensitive to reduced UPF1 levels than eIF4E-associated NMD. The residual ~10% of UPF1 protein in our knockdown experiments (Fig. 2a) appeared to be enough to occasionally target an eIF4E-bound NMD substrate during one of its multiple translation termination events. In contrast, only a few ribosomes are thought to be involved in the initial rounds of translation on CBC-bound mRNAs<sup>33</sup>, and the chance for UPF1 binding to a terminating ribosome becomes, therefore, disproportionately smaller under limiting UPF1 concentrations, resulting in greater NMD inhibition upon UPF1 knockdown. Consistent with this explanation, residual UPF1 still co-immunoprecipitated with eIF4E in UPF1 knockdown cells (Fig. 2a, lane 9).

We were surprised to observe that eIF4E-bound transcripts generally have a lower  $t_{1/2}$  than the corresponding transcripts in CBC-bound fractions (Figs. 2g,h and 3c,d). This was unexpected, given that the CBC-bound mRNA abundance decreases as a function not only of decay, but also of the replacement of CBC with eIF4E. The lower  $t_{1/2}$  of eIF4E-bound PTC+ transcripts might be due to the more efficient translation of these transcripts compared to CBC-associated mRNAs<sup>12</sup>, consistent with the direct relation between translation efficiency and the extent of NMD that has been reported<sup>44</sup>. The generally faster decay rate of eIF4E-bound transcripts might be a direct consequence of mRNA turnover through deadenylation, which is mediated by the PAN2–PAN3 and the CCR4–CAF1 complexes<sup>53</sup>. These factors are directly or indirectly recruited to the mRNP by PABPC1 (refs. 54,55). Compared to CBC-mRNPs, which carry a mixture of PABPC1 and PABPN1 on their poly(A) tails<sup>11,12</sup>, 4E-mRNPs have a higher relative abundance of PABPC1, which might lead to a more efficient recruitment of the deadenylation factors, resulting in faster decay. Furthermore, deadenylation has been linked to translation termination events<sup>54,55</sup>, and as translation termination events occur more frequently on eIF4E-bound transcripts, deadenylation might also occur more often, again resulting in a higher turnover rate.

Our demonstration that NMD can target mRNAs irrespectively of whether their cap is bound by CBC or eIF4E in mammalian cells is consistent with previous data from *S. cerevisiae*<sup>42,43</sup> and further corroborates the idea of an evolutionarily conserved mechanism of NMD substrate recognition<sup>56</sup>. In recent years, evidence has been accumulating that the triggering of NMD ultimately relies on competition between PABPC1 and UPF1 to interact with eRF3 at the terminating ribosome<sup>23,24</sup>. According to this model, eRF3–PABPC1 interaction is required for proper mRNA translation termination,

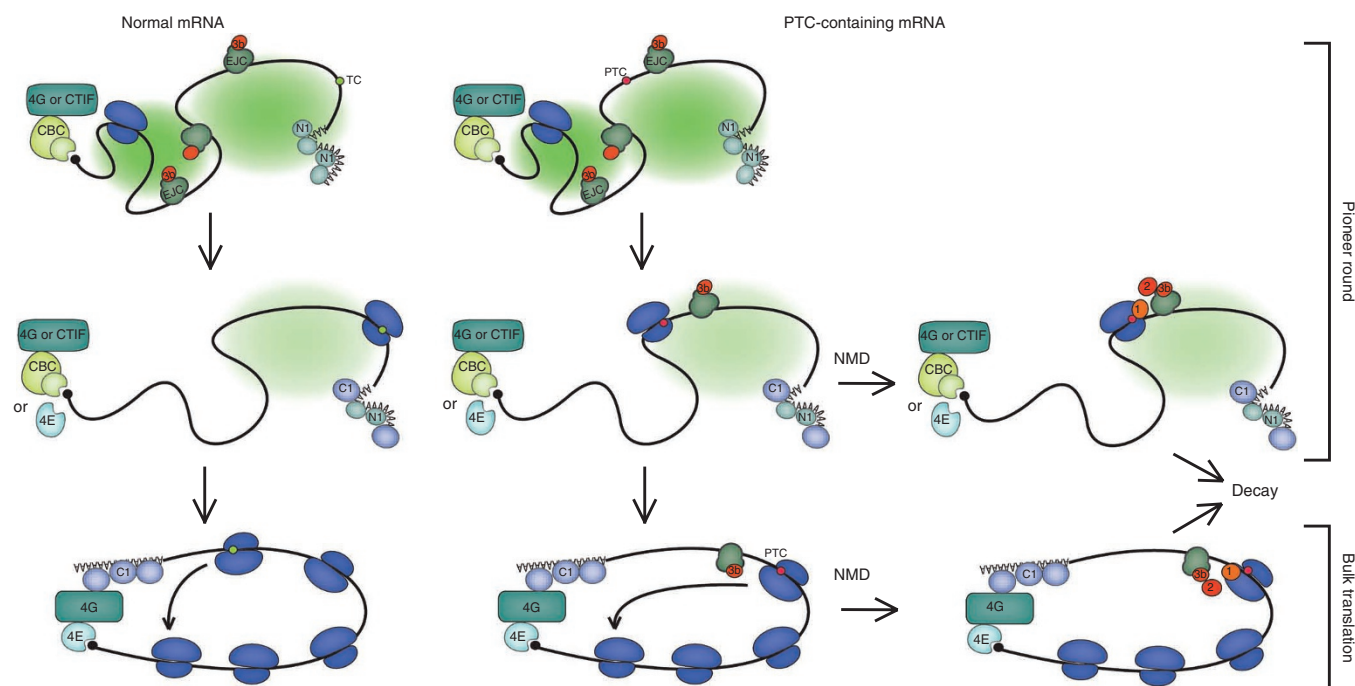


**Figure 4** NMD targets both CBC- and eIF4E-bound mRNAs: a graphical summary. The mRNP extrudes from the nucleus while still bound to the CBC. After entering the cytoplasm, the mRNP matures into a configuration competent for bulk translation. EJCs loaded in the ORF or <30 nt downstream of the stop codon are removed by the first ribosome, whereas the replacement of CBC by eIF4E occurs independently of translation. When the ORF is truncated by a PTC, the ribosome stalls for a prolonged time during translation termination, allowing UPF1 instead of PABPC1 to interact with eRF3, and NMD is induced. NMD can occur on CBC- or eIF4E-bound mRNA. 1, UPF1; 2, UPF2; 3b, UPF3B; 4E, eIF4E; 4G, eIF4G; N1, PABPN1; C1, PABPC1.

whereas the competing eRF3-UPF1 interaction leads to assembly of an NMD complex and subsequent degradation of the mRNA. This model implies that UPF1 and PABPC1 compete at every translation termination event and, thus, that NMD can occur during any round of translation. Our results confirm this prediction and fully support a model of aberrant translation termination leading to NMD. It is possible that the different protein composition of CBC-mRNPs and 4E-mRNPs could affect the proposed competition between PABPC1 and UPF1 for eRF3 binding. For example, the presence of PABPN1 on poly(A) tails of CBC-mRNPs reduces the number of bound PABPC1 molecules, which might shift the balance toward more efficient NMD with CBC-bound mRNAs.

EJCs enhance mammalian NMD efficiency by serving as a binding platform for the NMD factors UPF3B and UPF2 (refs. 24,57). That EJC factors can be readily detected in CBC-mRNPs but not in 4E-mRNPs in immunoprecipitation assays has been used as an argument for NMD's restriction to CBC-bound mRNA<sup>11,15,35</sup>. However, it is assumed that a large fraction of the mRNPs co-immunoprecipitating with CBC have not yet been translated and thus still contain all the originally deposited EJCs, explaining their high abundance in CBC-bound mRNPs (Fig. 4). In contrast, because EJCs are stripped off the mRNA by passing ribosomes, we expect only those located >30 nt downstream of premature or normal translation termination codons to persist on mRNAs after onset of translation and to have the potential to promote NMD at each termination event, even after the exchange of CBC for eIF4E. However, these remaining EJCs constitute only a small fraction of the EJCs originally present; hence, they cannot be detected in eIF4E immunoprecipitates.

Translation by the first ribosome causes extensive structural rearrangement of mRNPs<sup>14–16</sup>. Assuming that nascent mRNPs form a highly compact structure in the nucleus that may be important

for their export to the cytoplasm<sup>2</sup>, we assume also that they must decondense during the initial round of translation to eventually adopt a conformation that allows efficient eIF4E-mediated bulk translation (Fig. 4). Because the exchange of CBC for eIF4E is a translation-independent process<sup>14</sup>, there is no reason to assume that the first round of translation could not take place on mRNPs that contain eIF4E at the cap. Notably, even 12 h after transcription inhibition, we still detected a considerable fraction of CBP80-bound miniμ wild-type NFB reporter mRNA, suggesting that some mRNAs may never exchange CBC for eIF4E.

It is well documented that eIF4E interacts with eIF4G, which in turn binds to PABPC1, leading to mRNA circularization by positioning of the capped 5' end close to the poly(A) tail<sup>46,47</sup>. This circularization has been shown to positively affect eIF4E-mediated translation<sup>46,47,58</sup>. Although eIF4G, eIF4A, PABPC1 and eIF2 $\alpha$  have also been detected in CBC-mRNPs and suggested to promote translation initiation and termination<sup>12</sup>, CBC-mRNPs do not seem to form an analogous circular structure, as indicated by the loss of CBP80 interaction with both PABPC1 and PABPN1 upon RNA digestion (Fig. 1a and Supplementary Fig. 1a). This apparent lack of physical link between the CBC-bound 5' end and the 3' end of mRNA could be due either to the absence of the bridging factor eIF4G in CBC-mRNPs or to the presence of PABPN1 on the poly(A) tail of CBC-mRNPs, which might negatively affect the eIF4G-PABPC1 interaction (Fig. 4). The data as to whether eIF4G is involved in CBC-associated translation are contradictory. On one hand, CBC and eIF4G interact *in vitro* and co-immunoprecipitate from cell lysates<sup>48,49</sup>. On the other hand, we and others have not been able to consistently detect eIF4G in CBP80 immunoprecipitates<sup>36</sup> (Figs. 1a and 2a), and the CBC-dependent translation initiation factor CTIF has been reported to substitute for eIF4G in translation of CBC-associated mRNAs by binding to CBP80

(ref. 36). However, we could not detect CTIF in our CBC-mRNPs (Supplementary Fig. 1b), and knockdown of CTIF did not stabilize the mRNA of TCR- $\beta$  ter68 (data not shown). We cannot rule out the possibility that the low immunoprecipitation efficiency was responsible for the apparent absence of CTIF and eIF4G in our CBP80 immunoprecipitates. Thus, the exact roles of eIF4G and CTIF in translation of CBC-bound mRNA remain to be clarified.

In conclusion, our results demonstrate that NMD is not restricted to CBC-bound mRNPs in mammalian cells and that NMD can act during any round of translation. Until now, the exact role of CBC-mediated translation has not been fully understood, and its significance for downstream processes, including eIF4E-mediated translation, needs additional investigation. To further address this question, the development of approaches allowing specific inhibition of CBC-associated translation will be required.

## METHODS

Methods and any associated references are available in the [online version of the paper](#).

Note: Supplementary information is available in the [online version of the paper](#).

## ACKNOWLEDGMENTS

We thank E. Izaurralde (Max Planck Institute), N. Sonenberg (McGill University) and Y.-K. Kim (Korea University) for antibodies, and J. Lykke-Andersen and A. Jacobson for valuable comments on the manuscript. This work was supported by grants of the European Research Council (StG 207419; O.M.), the Swiss National Science Foundation (31003A-127614 and 31003A-143717; O.M.) and the canton of Bern.

## AUTHOR CONTRIBUTIONS

S.C.R. and O.M. conceived of and designed the experiments. S.C.R. performed the experiments. O.M. and S.C.R. wrote the paper. O.M. provided resources.

## COMPETING FINANCIAL INTERESTS

The authors declare no competing financial interests.

Reprints and permissions information is available online at <http://www.nature.com/reprints/index.html>.

- Moore, M.J. & Proudfoot, N.J. Pre-mRNA processing reaches back to transcription and ahead to translation. *Cell* **136**, 688–700 (2009).
- Singh, G. *et al.* The cellular EJC interactome reveals higher-order mRNP structure and an EJC-SR protein nexus. *Cell* **151**, 750–764 (2012).
- Izaurralde, E. *et al.* A nuclear cap binding protein complex involved in pre-mRNA splicing. *Cell* **78**, 657–668 (1994).
- Visa, N., Izaurralde, E., Ferreira, J., Daneholt, B. & Mattaj, I.W. A nuclear cap-binding complex binds Balbiani ring pre-mRNA cotranscriptionally and accompanies the ribonucleoprotein particle during nuclear export. *J. Cell Biol.* **133**, 5–14 (1996).
- Le Hir, H., Izaurralde, E., Maquat, L.E. & Moore, M.J. The spliceosome deposits multiple proteins 20–24 nucleotides upstream of mRNA exon-exon junctions. *EMBO J.* **19**, 6860–6869 (2000).
- Saulière, J. *et al.* CLIP-seq of eIF4AIII reveals transcriptome-wide mapping of the human exon junction complex. *Nat. Struct. Mol. Biol.* **19**, 1124–1131 (2012).
- Baltz, A.G. *et al.* The mRNA-bound proteome and its global occupancy profile on protein-coding transcripts. *Mol. Cell* **46**, 674–690 (2012).
- Castello, A. *et al.* Insights into RNA biology from an atlas of mammalian mRNA-binding proteins. *Cell* **149**, 1393–1406 (2012).
- Keene, J.D. RNA regulons: coordination of post-transcriptional events. *Nat. Rev. Genet.* **8**, 533–543 (2007).
- Fortes, P. *et al.* The yeast nuclear cap binding complex can interact with translation factor eIF4G and mediate translation initiation. *Mol. Cell* **6**, 191–196 (2000).
- Ishigaki, Y., Li, X.J., Serin, G. & Maquat, L.E. Evidence for a pioneer round of mRNA translation: mRNAs subject to nonsense-mediated decay in mammalian cells are bound by CBP80 and CBP20. *Cell* **106**, 607–617 (2001).
- Chiu, S.Y., Lejeune, F., Ranganathan, A.C. & Maquat, L.E. The pioneer translation initiation complex is functionally distinct from but structurally overlaps with the steady-state translation initiation complex. *Genes Dev.* **18**, 745–754 (2004).
- Maquat, L.E. Nonsense-mediated mRNA decay: Splicing, translation and mRNP dynamics. *Nat. Rev. Mol. Cell Biol.* **5**, 89–99 (2004).
- Sato, H. & Maquat, L.E. Remodeling of the pioneer translation initiation complex involves translation and the karyopherin importin beta. *Genes Dev.* **23**, 2537–2550 (2009).
- Lejeune, F., Ishigaki, Y., Li, X.J. & Maquat, L.E. The exon junction complex is detected on CBP80-bound but not eIF4E-bound mRNA in mammalian cells: dynamics of mRNP remodeling. *EMBO J.* **21**, 3536–3545 (2002).
- Dostie, J. & Dreyfuss, G. Translation is required to remove Y14 from mRNAs in the cytoplasm. *Curr. Biol.* **12**, 1060–1067 (2002).
- Dias, S.M., Wilson, K.F., Rojas, K.S., Ambrosio, A.L. & Cerione, R.A. The molecular basis for the regulation of the cap-binding complex by the importins. *Nat. Struct. Mol. Biol.* **16**, 930–937 (2009).
- Görlich, D. *et al.* Importin provides a link between nuclear protein import and U snRNA export. *Cell* **87**, 21–32 (1996).
- Blachut-Okrasińska, E. *et al.* Stopped-flow and Brownian dynamics studies of electrostatic effects in the kinetics of binding of 7-methyl-GpppG to the protein eIF4E. *Eur. Biophys. J.* **29**, 487–498 (2000).
- Worch, R. *et al.* Diverse role of three tyrosines in binding of the RNA 5' cap to the human nuclear cap binding complex. *J. Mol. Biol.* **385**, 618–627 (2009).
- Haghighat, A. & Sonenberg, N. eIF4G dramatically enhances the binding of eIF4E to the mRNA 5'-cap structure. *J. Biol. Chem.* **272**, 21677–21680 (1997).
- Gross, J.D. *et al.* Ribosome loading onto the mRNA cap is driven by conformational coupling between eIF4G and eIF4E. *Cell* **115**, 739–750 (2003).
- Kervestin, S. & Jacobson, A. NMD: a multifaceted response to premature translational termination. *Nat. Rev. Mol. Cell Biol.* **13**, 700–712 (2012).
- Schweingruber, C., Rufener, S.C., Zünd, D., Yamashita, A. & Mühlemann, O. Nonsense-mediated mRNA decay—mechanisms of substrate mRNA recognition and degradation in mammalian cells. *Biochim. Biophys. Acta* <http://dx.doi.org/10.1016/j.bbaggm.2013.02.005> (20 February 2013).
- Kashima, I. *et al.* Binding of a novel SMG-1-Upf1-eRF1-eRF3 complex (SURF) to the exon junction complex triggers Upf1 phosphorylation and nonsense-mediated mRNA decay. *Genes Dev.* **20**, 355–367 (2006).
- Stalder, L. & Mühlemann, O. The meaning of nonsense. *Trends Cell Biol.* **18**, 315–321 (2008).
- Okada-Katsuhata, Y. *et al.* N- and C-terminal Upf1 phosphorylations create binding platforms for SMG-6 and SMG-5:SMG-7 during NMD. *Nucleic Acids Res.* **40**, 1251–1266 (2012).
- Chakrabarti, S. *et al.* Molecular mechanisms for the RNA-dependent ATPase activity of Upf1 and its regulation by Upf2. *Mol. Cell* **41**, 693–703 (2011).
- Arias-Palomo, E. *et al.* The nonsense-mediated mRNA decay SMG-1 kinase is regulated by large-scale conformational changes controlled by SMG-8. *Genes Dev.* **25**, 153–164 (2011).
- Ohnishi, T. *et al.* Phosphorylation of hUPF1 induces formation of mRNA surveillance complexes containing hSMG-5 and hSMG-7. *Mol. Cell* **12**, 1187–1200 (2003).
- Fukuhara, N. *et al.* SMG7 is a 14–3-3-like adaptor in the nonsense-mediated mRNA decay pathway. *Mol. Cell* **17**, 537–547 (2005).
- Cho, H., Kim, K.M. & Kim, Y.K. Human proline-rich nuclear receptor coregulatory protein 2 mediates an interaction between mRNA surveillance machinery and decapping complex. *Mol. Cell* **33**, 75–86 (2009).
- Maquat, L.E., Tarn, W.Y. & Isken, O. The pioneer round of translation: features and functions. *Cell* **142**, 368–374 (2010).
- Hwang, J., Sato, H., Tang, Y.L., Matsuda, D. & Maquat, L.E. UPF1 association with the cap-binding protein, CBP80, promotes nonsense-mediated mRNA decay at two distinct steps. *Mol. Cell* **39**, 396–409 (2010).
- Hosoda, N., Kim, Y.K., Lejeune, F. & Maquat, L.E. CBP80 promotes interaction of Upf1 with Upf2 during nonsense-mediated mRNA decay in mammalian cells. *Nat. Struct. Mol. Biol.* **12**, 893–901 (2005).
- Kim, K.M. *et al.* A new MIF4G domain-containing protein, CTIF, directs nuclear cap-binding protein CBP80/20-dependent translation. *Genes Dev.* **23**, 2033–2045 (2009).
- Oh, N., Kim, K.M., Cho, H., Choe, J. & Kim, Y.K. Pioneer round of translation occurs during serum starvation. *Biochem. Biophys. Res. Commun.* **362**, 145–151 (2007).
- Oh, N., Kim, K.M., Choe, J. & Kim, Y.K. Pioneer round of translation mediated by nuclear cap-binding proteins CBP80/20 occurs during prolonged hypoxia. *FEBS Lett.* **581**, 5158–5164 (2007).
- Schoenberg, D.R. & Maquat, L.E. Regulation of cytoplasmic mRNA decay. *Nat. Rev. Genet.* **13**, 246–259 (2012).
- Chang, Y.F., Imam, J.S. & Wilkinson, M.E. The nonsense-mediated decay RNA surveillance pathway. *Annu. Rev. Biochem.* **76**, 51–74 (2007).
- Hogg, J.R. & Goff, S.P. Upf1 senses 3' UTR length to potentiate mRNA decay. *Cell* **143**, 379–389 (2010).
- Maderazo, A.B., Belk, J.P., He, F. & Jacobson, A. Nonsense-containing mRNAs that accumulate in the absence of a functional nonsense-mediated mRNA decay pathway are destabilized rapidly upon its restitution. *Mol. Cell Biol.* **23**, 842–851 (2003).
- Gao, Q., Das, B., Sherman, F. & Maquat, L.E. Cap-binding protein 1-mediated and eukaryotic translation initiation factor 4E-mediated pioneer rounds of translation in yeast. *Proc. Natl. Acad. Sci. USA* **102**, 4258–4263 (2005).
- Gaba, A., Jacobson, A. & Sachs, S.S. Ribosome occupancy of the yeast CPA1 upstream open reading frame termination codon modulates nonsense-mediated mRNA decay. *Mol. Cell* **20**, 449–460 (2005).
- Calero, G. *et al.* Structural basis of m<sup>7</sup>GpppG binding to the nuclear cap-binding protein complex. *Nat. Struct. Biol.* **9**, 912–917 (2002).
- Wells, S.E., Hillner, P.E., Vale, R.D. & Sachs, A.B. Circularization of mRNA by eukaryotic translation initiation factors. *Mol. Cell* **2**, 135–140 (1998).

47. Imataka, H., Gradi, A. & Sonenberg, N. A newly identified N-terminal amino acid sequence of human eIF4G binds poly(A)-binding protein and functions in poly(A)-dependent translation. *EMBO J.* **17**, 7480–7489 (1998).
48. McKendrick, L., Thompson, E., Ferreira, J., Morley, S.J. & Lewis, J.D. Interaction of eukaryotic translation initiation factor 4G with the nuclear cap-binding complex provides a link between nuclear and cytoplasmic functions of the m<sup>7</sup> guanosine cap. *Mol. Cell Biol.* **21**, 3632–3641 (2001).
49. Lejeune, F., Ranganathan, A.C. & Maquat, L.E. eIF4G is required for the pioneer round of translation in mammalian cells. *Nat. Struct. Mol. Biol.* **11**, 992–1000 (2004).
50. Eberle, A.B., Stalder, L., Mathys, H., Orozco, R.Z. & Mühlemann, O. Posttranscriptional gene regulation by spatial rearrangement of the 3' untranslated region. *PLoS Biol.* **6**, e92 (2008).
51. Mili, S. & Steitz, J.A. Evidence for reassociation of RNA-binding proteins after cell lysis: implications for the interpretation of immunoprecipitation analyses. *RNA* **10**, 1692–1694 (2004).
52. Bühler, M., Steiner, S., Mohn, F., Paillusson, A. & Mühlemann, O. EJC-independent degradation of nonsense immunoglobulin- $\mu$  mRNA depends on 3' UTR length. *Nat. Struct. Mol. Biol.* **13**, 462–464 (2006).
53. Yamashita, A. *et al.* Concerted action of poly(A) nucleases and decapping enzyme in mammalian mRNA turnover. *Nat. Struct. Mol. Biol.* **12**, 1054–1063 (2005).
54. Funakoshi, Y. *et al.* Mechanism of mRNA deadenylation: evidence for a molecular interplay between translation termination factor eRF3 and mRNA deadenylases. *Genes Dev.* **21**, 3135–3148 (2007).
55. Ruan, L. *et al.* Quantitative characterization of Tob interactions provides the thermodynamic basis for translation termination-coupled deadenylase regulation. *J. Biol. Chem.* **285**, 27624–27631 (2010).
56. Mühlemann, O. Recognition of nonsense mRNA: towards a unified model. *Biochem. Soc. Trans.* **36**, 497–501 (2008).
57. Chamieh, H., Ballut, L., Bonneau, F. & Herve, L.H. NMD factors UPF2 and UPF3 bridge UPF1 to the exon junction complex and stimulate its RNA helicase activity. *Nat. Struct. Mol. Biol.* **15**, 85–93 (2008).
58. Kahvejian, A., Svitkin, Y.V., Sukarieh, R., M'Boutchou, M.N. & Sonenberg, N. Mammalian poly(A)-binding protein is a eukaryotic translation initiation factor, which acts via multiple mechanisms. *Genes Dev.* **19**, 104–113 (2005).

## ONLINE METHODS

**Plasmids.** The TCR- $\beta$  fragments of p $\beta$ -510 (wild-type version; ref. 59) and  $\beta$ -610 (ter68 version) were inserted between Kpn1 and BamH1 sites of the pTRE tight vector (Clontech). The pTRE tight-mini $\mu$  C3/H4 foldback constructs have been described previously<sup>50</sup>. For knockdown experiments, pSUPuro plasmids expressing short hairpin RNAs (shRNAs) were used<sup>59</sup>. Target sequences are provided in **Supplementary Table 1**.

**Cell lines.** HeLa Tet-Off cells<sup>50</sup>, which express the stably integrated tTA-Advanced gene (Clontech), were used to generate clonal cell lines stably transfected with either the TCR- $\beta$  wild-type or TCR- $\beta$  ter68 minigene or polyclonal cell pools stably expressing mini $\mu$  wild-type NFB, mini $\mu$  ter440 FB or mini $\mu$  ter440 NFB. For production of all cell lines, linearized pTRE tight plasmids encoding the respective reporter constructs were co-transfected with a blasticidin resistance gene-containing DNA fragment at a molar ratio of 1:10. Starting 2 d after transfection, cells were selected with increasing amounts of blasticidin (1–3  $\mu$ g/ml) for 3 weeks. From the TCR- $\beta$ -expressing cell pools, clonal cell lines were derived by single-cell dilution.

**Cell culture, transient transfection and drug treatment.** Cells were cultured in DMEM (Invitrogen) supplemented with 10% FCS (Invitrogen) or tetracycline-free (tet-free) FCS (Amimed), 100 U/ml penicillin (Invitrogen) and 100  $\mu$ g/ml streptomycin (Invitrogen). The cells were incubated at 37 °C in humid atmosphere containing 5% CO<sub>2</sub>.

For immunoprecipitation experiments in combination with UPF1 knockdown, transfections were performed in 150-mm cell culture dishes. Cells ( $2.5 \times 10^6$ ) were seeded then transfected the next day with 5  $\mu$ g of pSUPuro plasmid<sup>59</sup> and 30  $\mu$ L of DreamFect (OZ Biosciences) according to the manufacturer's protocol. One day after transfection (d.p.t.), cells were treated with 1.5  $\mu$ g puromycin per milliliter of medium for 2 d to eliminate untransfected cells. The cells were then cultured in puromycin-free medium for another day before production of cell extracts. For transcript half-life determination experiments, two 150-mm dishes were pooled after 2 d of puromycin selection, split into five 150-mm dishes and cultured in antibiotic-free medium for another day. Time course was started 4 d.p.t. by adding 1  $\mu$ g doxycycline (dox; Sigma-Aldrich) per milliliter of medium to each dish at different time points (8, 5 and 3 h before harvesting). The cells were then harvested, and immunoprecipitation experiments were performed as described below. In time-course experiments without knockdown, dox was added to a final concentration of 1  $\mu$ g/mL to untransfected cells 12, 8 and 4 h before harvesting.

To determine the leakiness of the Tet-Off system in the different cell lines, cells were incubated with 1  $\mu$ g dox per milliliter of medium for 96 h (dox-containing medium was replaced every 48 h). Cells were harvested and subjected to immunoprecipitation experiments as described below.

**Preparation of cell extracts.** For immunoprecipitation experiments,  $6 \times 10^6$  cells (half of a 150-mm cell cultured dish) were lysed for 30 min at 4 °C in 600  $\mu$ L of either RNA-IP lysis buffer (50 mM Tris-HCl (pH 7.8), 150 mM NaCl, 1 mM EDTA, 1% Triton X-100 in diethylpyrocarbonate (DEPC)-treated H<sub>2</sub>O; for CBP80 and eIF4E, immunoprecipitations (IPs)) or hypotonic gentle lysis buffer (10 mM Tris-HCl (pH 7.5), 10 mM NaCl, 2 mM EDTA, 0.5% Triton X-100 in DEPC-treated H<sub>2</sub>O, for eIF4E IPs) supplemented with 1 $\times$  proteinase inhibitor (Thermo Scientific) and 24 U RiboLock RNase Inhibitor (Fermentas). For RNase treatments, RNase A (Sigma-Aldrich) was added to a final concentration of 200  $\mu$ g/mL, and RNase inhibitor was omitted. When gentle hypotonic lysis buffer was used, NaCl was added to a final concentration of 140 mM after 20 min of incubation. Lysates were then centrifuged for 10 min at 4 °C and 12,000g, and the supernatants were recovered.

**RNA immunoprecipitation with non-cross-linked cells.** Cells were transfected, drug treated, harvested and lysed as described above. For half-life experiments, cells from one 150-mm cell culture dish were divided equally and subjected to either anti-CBP80 or anti-eIF4E immunoprecipitations. For the input controls, lysate corresponding to 10% of the material used for the immunoprecipitations was set aside. To the input aliquot for protein analysis, 2 $\times$  SDS-PAGE loading buffer (60 mM Tris-HCl (pH 6.6), 200 mM DTT, 10% (v/v) glycerol, 2% (w/v)

SDS, 0.01% (w/v) bromophenol blue) was added, and the aliquot for RNA analysis received TRI-Reagent (800 mM guanidine thiocyanate, 400 mM ammonium thiocyanate, 100 mM sodium acetate, 5% (v/v) glycerol, 38% (v/v) saturated phenol). The aliquots were stored at –20 °C until use.

For the immunoprecipitations, 2–4  $\mu$ g rabbit anti-CBP80 (Bethyl; A301-794A) or 2–5  $\mu$ g mouse anti-eIF4E (Santa Cruz; sc-9976) or the corresponding amount of normal rabbit or mouse IgG (Santa Cruz; sc-2027 and sc-2025) were incubated with a 30- $\mu$ L Dynabeads slurry (Life Technologies) in a total volume of 100  $\mu$ L IIP150-NP40 (10 mM Tris-HCl (pH 7.8), 150 mM NaCl, 0.1% Nonidet P-40 (NP-40) in DEPC-treated H<sub>2</sub>O) for 2 h at 4 °C on a rotating wheel. The beads were then washed three times in IIP150-NP40 using the magnetic rack (Life Technologies) and subsequently incubated with 500  $\mu$ L cell lysate for 2 h at 4 °C. Then the beads were washed five times in IIP150-NP40 supplemented with 20 U/mL RiboLock RNase Inhibitor (Fermentas) and transferred to a fresh tube. After all buffer fluid was removed, the beads were resuspended in 2 $\times$  SDS-PAGE loading buffer. When both protein and RNA analysis was required, the beads were split in a 1:1 or 2:3 ratio, and 2 $\times$  SDS-PAGE loading buffer was added to the former fraction and TRI-reagent was added to the latter. Protein samples from input and immunoprecipitations were incubated at 95 °C for 5 min before loading on the SDS-PAGE.

**Reverse transcription.** RNA isolation was generally followed by ethanol precipitation at –20 °C overnight. For the input samples, usually, 600 ng of RNA from whole-cell extracts were reverse transcribed as described previously<sup>60</sup>. The immunoprecipitated RNA was reverse transcribed in a total volume of 50  $\mu$ L under the same conditions.

**Quantitative real-time PCR.** Reverse-transcribed material corresponding to 24 ng of RNA (or 3–4% of the immunoprecipitated RNA) was amplified in Brilliant III Ultra-Fast qPCR Master Mix (Agilent Technologies) in a total volume of 15  $\mu$ L with the Rotor-Gene 6000 rotary analyzer (Corbett). Primer and probe sequences are listed in **Supplementary Table 2**. The following two-step cycling protocol was used: initial denaturation at 95 °C for 3 min; 40 cycles of 95 °C for 5 s; 60 °C for 15 s.

**Calculation of half-lives and applied statistics.** To calculate the exponential mRNA decay, the experimentally determined background generated by leakiness of the Tet-Off system (see above) was subtracted from all mRNA measurements of every experiment using the formula  $A = (B - x) / (100 - x) \times 100$ , where  $A$  represents the background-corrected relative mRNA level,  $B$  is the relative mRNA level before background subtraction and  $x$  is the measured background level of the corresponding cell line minus 1. The zero baseline of the exponential decay was set to 1, and measurements <1 were regarded as background. For the decay graphs, the relative mRNA levels from all experiments for each time point were averaged, and s.d. was calculated. The half-life of every single experiment was calculated in Excel (Microsoft Corporation) using the LOGEST function to determine the decay constant  $\lambda$  and the half-life  $t_{1/2} = \ln 2 / \lambda$ . Half-lives from at least three biologically independent experiments were averaged, and the s.d. was determined.  $P$  values were calculated in Excel using the two-sample equal variance (homoscedastic), one-sided Student's  $t$ -test.

**PCR.** To test the efficiency of the RNase treatment, the same volume of RNase-treated and control RNA samples from whole-cell extracts were used for reverse transcription. Reverse-transcribed material corresponding to 24 ng of RNA was amplified in a total volume of 20  $\mu$ L using the Maximo Taq Faststart PCR mix (GeneOn) and 1  $\mu$ M each of forward and reverse primers. Primer sequences are listed in **Supplementary Table 2**. A three-step cycling protocol was used: initial denaturation at 95 °C for 5 min; 31 cycles of 95 °C for 45 s; 58 °C for 1 min and 72 °C for 1.5 min. PCR was finished by 72 °C for 10 min. Ten microliters of each reaction were analyzed on a 1% agarose gel.

**Immunoblotting.** As input samples, whole-cell extracts corresponding to  $4 \times 10^4$  to  $4.5 \times 10^5$  cells per lane were loaded. For the immunoprecipitations, 25–50% of the total immunoprecipitates were run on an 8%, 10%, 12% or 15% SDS-PAGE. Proteins were transferred to Optitrans BA-S 85 reinforced nitrocellulose (Whatman) and probed at 4 °C overnight with the following antibodies: goat anti-UPF1 (Bethyl; A300-038A, diluted 1:1,000), rabbit anti-ACTIN

(Sigma-Aldrich; A5060, diluted 1:2,000), rabbit anti-CBP80 (gift from E. Izaurralde<sup>3</sup>, diluted 1:2,000), rabbit anti-eIF4E (Bethyl; A301-154A, diluted 1:1,000), rabbit anti-eIF4G (gift from N. Sonenberg, diluted 1:1,000), mouse anti-PABPC1 (Sigma-Aldrich; P6246, diluted 1:1,000), rabbit anti-CTIF (gift from Y.K. Kim, diluted 1:1,000)<sup>36</sup> or rabbit anti-Flag (Antikoerper-online; ABIN99294, diluted 1:2,000). Donkey anti-rabbit IRDye 800CW, donkey anti-mouse IRDye 800CW, donkey anti-goat IREDye 800CW and donkey anti-mouse IREDye 680LT (all from Li-Cor; Lincoln, NE, diluted 1:10,000) were used as secondary antibodies

(1 h incubation at room temperature). Fluorescent signals were visualized by scanning the membrane on an Odyssey Infrared Imager (Li-Cor).

59. Paillusson, A., Hirschi, N., Vallan, C., Azzalin, C.M. & Mühlemann, O. A GFP-based reporter system to monitor nonsense-mediated mRNA decay. *Nucleic Acids Res.* **33**, e54 (2005).
60. Yepiskoposyan, H., Aeschmann, F., Nilsson, D., Okoniewski, M. & Mühlemann, O. Autoregulation of the nonsense-mediated mRNA decay pathway in human cells. *RNA* **17**, 2108–2118 (2011).